

Subsampling Spectral Clustering for Stochastic Block Models in Large-Scale Networks

Jiayi Deng^{1,2}, Yi Ding^{1,2}, Yingqiu Zhu³, and Danyang Huang^{1,2*}, Bingyi Jing⁴, and Bo Zhang^{1,2*}

¹ *Center for Applied Statistics, Renmin University of China, Beijing, China;*

² *School of Statistics, Renmin University of China, Beijing, China;*

³ *School of Statistics, University of International Business and Economics;*

⁴ *The Hong Kong University of Science and Technology, Hong Kong, China.*

Abstract

The rapid development of science and technology has generated large amounts of network data, leading to significant computational challenges for network community detection. Here, we propose a novel subsampling spectral clustering algorithm to identify community structures in large-scale networks with limited computing resources. More precisely, spectral clustering is conducted using only the information of a small subsample of the network nodes, resulting in a huge reduction in computational time. As a result, for large-scale datasets, the method can be realized even using a personal computer. Specifically, we introduce two different sampling techniques, namely simple random subsampling and degree corrected subsampling. The theoretical properties of these two subsampling algorithms for spectral clustering are then established accordingly. Finally, to illustrate and evaluate the proposed method, a number of simulation studies and a real data analysis are conducted.

KEY WORDS: Large-scale Networks; Community Detection; Subsampling; Spectral Clustering

*Danyang Huang and Bo Zhang are co-corresponding authors. They have contributed equally to this paper. Danyang Huang, Center for Applied Statistics, School of Statistics, Renmin University of China at Beijing, 59 Zhongguancun Street, 100872, China; dyhuang@ruc.edu.cn. Bo Zhang, Center for Applied Statistics, School of Statistics, Renmin University of China at Beijing, 59 Zhongguancun Street, 100872, China; mabzhang@ruc.edu.cn. This work was supported by the National Natural Science Foundation of China (grant numbers 12071477, 11701560, 71873137); fund for building world-class universities (disciplines) of Renmin University of China. The authors gratefully acknowledge the support of Public Computing Cloud, Renmin University of China.

1. INTRODUCTION

Community detection is an important research direction in network analysis (Newman and Girvan, 2004; Fortunato, 2010), and it aims to cluster the nodes into different groups with high edge concentrations within the same cluster and low concentrations between different ones (Girvan and Newman, 2002; Lancichinetti and Fortunato, 2009). Network community detection is widely applied in various research areas, including, but not being limited to, computer science (Agarwal et al., 2005; Tron and Vidal, 2007), social science (Zhao et al., 2011; Lee et al., 2017), and biology (Rives and Galitski, 2003; Chen and Yuan, 2006; Nepusz et al., 2012). Recently, the advances of science and technology created large amounts of online network data. However, even if the computing techniques have improved significantly, directly dealing with large-scale network data remains challenging, especially when available computing resources are limited (Harenberg et al., 2014; Wang et al., 2018, 2019).

In community detection literature, spectral clustering is one of the most popular methods because it is easy to implement and has well-founded theoretical guarantees (Ng et al., 2002; Rohe et al., 2011; Krzakala et al., 2013; Binkiewicz et al., 2017). Given a network with N nodes and K different clusters, spectral clustering embeds each node in a K -dimensional space based on singular value decomposition (SVD). The computational complexity of spectral clustering is $O(N^3)$ if a full SVD is performed (Yan et al., 2009; Li et al., 2011; Chen and Cai, 2011), which is difficult to afford for large-scale networks to afford. For example, as shown in Figure 5, conducting spectral clustering for $N = 10,000$ nodes will cost 298.446 seconds for a personal computer with a 3.70 GHz Intel Core i9 processor. For a larger $N = 30,000$, the time cost increases sharply to 6,600.103 seconds. Therefore, using spectral clustering to identify the community structures of large networks presents huge computational challenges.

There has been an increasing interest in studying fast spectral clustering for large-scale networks. For example, [Yan et al. \(2009\)](#) developed a fast approximate of spectral clustering by local data reduction, which replaces the original dataset with a small number of representative points. [Chen et al. \(2010\)](#) proposed the parallel spectral clustering method that first constructs a sparse similarity matrix and then calculates the embedding vector of each point in parallel. In addition, [Chen and Cai \(2011\)](#) developed the landmark-based spectral clustering, which selects a few representative points as landmarks and represents the original data points as a linear combination of these landmarks. To speed up the eigendecomposition, several researchers exploited the numerical solution of eigenfunction problems, the Nyström method ([Fowlkes et al., 2004](#); [Drineas and Mahoney, 2005](#)). More recently, many fast SVD algorithms using randomization techniques have been proposed, including [Halko et al. \(2011\)](#); [Feng et al. \(2018\)](#); [Martin et al. \(2018\)](#); [Zhang et al. \(2022\)](#). However, the computational complexity of these methods is in the order of $O(N^2)$. Such computational costs are still intractable for many real-world applications. This motivates us to extend the traditional spectral clustering under the constraint of limited computing resources.

We investigate selecting a small node set to extract the network structure information with limited computational cost. Considering large-scale networks, the network structure information is contained in the connections among nodes and can be represented by network adjacency or Laplacian matrices. However, such matrices are high-dimensional and could lead to high computational costs. To solve the problem, we propose selecting a small node set and then consider extracting the network community structure only through connections related to the selected nodes. To illustrate, we provide an example of network subsampling as shown in [Figure 1](#), where the graph contains ten nodes assigned to two communities. It is remarkable that we can perfectly

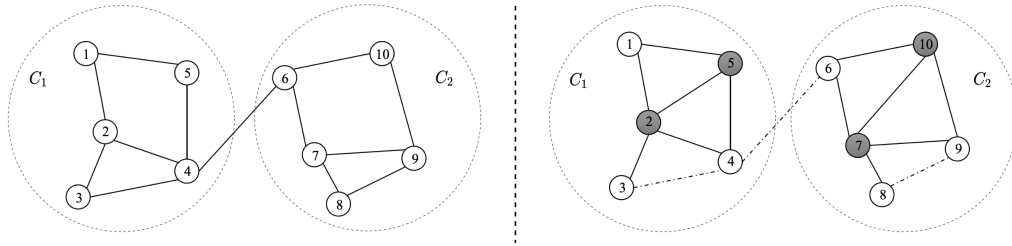


Figure 1: Example of network subsampling. A network with ten nodes and two communities (C_1, C_2) is displayed in the left panel. The right panel is a subgraph, in which the selected nodes are gray, the edges connected by selected nodes are indicated by solid lines, and the edges between unselected nodes are denoted by dashed lines.

identify the community labels for all nodes based only on the connections related to the selected nodes. Moreover, because we only select a small subset of the total nodes, we can use a much lower dimensional matrix to represent the network nodes' connection information.

In this way, we propose a subsampling spectral clustering (SSC) method for large-scale networks under the constraint of limited computing resources. To the best of our knowledge, this is the first study to discuss network subsampling for community detection in large-scale networks. Specifically, we discuss two types of subsampling methods: simple random subsampling (SRS) and degree-corrected subsampling (DCS). To evaluate the efficiency of the SSC method, we apply it to a dataset with $N = 9,980$ nodes collected from Sina Weibo. As shown in Section 4.3, when the subsample size is 200 nodes, the SSC method is about 443 (298.827s / 0.674s) times faster than traditional spectral clustering, but there is little loss of accuracy. Additionally, we provide theoretical guarantees for the SSC method. Specifically, we prove that subsampling size n can be as small as $\Omega\{\log(N)\}$ based on the stochastic block model (SBM) (Holland et al., 1983). We then show that the computational complexity of the SSC method could be as small as $O(n^2N)$. It is noteworthy that $n \ll N$, which implies that the computational complexity of the proposed method could be as low as $O(N\{\log(N)\}^2)$.

The remainder of the paper is organized as follows. In Section 2, we propose the SSC algorithm and discuss the two subsampling methods. In Section 3, we establish the theoretical properties of the two subsampling methods. The simulation and real data studies are presented in Section 4. Section 5 highlights the main conclusions and discusses future research. All technical proofs are presented in the Appendices of the Supplementary Material.

2. SUBSAMPLING SPECTRAL CLUSTERING FOR STOCHASTIC BLOCK MODELS

Here, we propose a spectral clustering method based on subsampling and introduce two different subsampling methods for spectral clustering in the SBM theoretical framework. The stochastic block model is an important random graph model for studying community detection (Holland et al., 1983; Rohe et al., 2011). Let $\text{Bern}(p)$ be the Bernoulli distribution with success probability $p \in [0, 1]$. Under a SBM with N nodes and K communities, define a symmetric probability matrix $B = (B_{kk'}) \in [0, 1]^{K \times K}$ and a label vector $z = (z_1, \dots, z_N)^\top \in [K]^N$. Here, $[K] = \{1, \dots, K\}$ and then its adjacency matrix $A = (A_{ij}) \in \{0, 1\}^{N \times N}$ is assumed to be symmetric with zero diagonals and, for all $i > j$, $A_{ij} = A_{ji} \sim \text{Bern}(B_{z_i z_j})$ independently. It is noteworthy that, for any $i, j \in [N]$, the probability of an edge between node i and j depends only on their community memberships. Further, we define \mathcal{G} as an undirected graph generated from the SBM.

2.1. Subsampling Spectral Clustering

We propose the SSC method in a large-scale network based on the SBM theoretical framework. Owing to computational complexity considerations, we first subsample a

sub-vertex set V_s from the graph \mathcal{G} and then identify network communities using a spectral method to the subsampled Laplacian matrix.

Specifically, given network \mathcal{G} , let $V_s = \{s_j : s_j \in [N], 1 \leq j \leq n\}$, where s_j denotes the selected node. Moreover, we define a bi-adjacency matrix $A^s = (A_{ij}^s) \in \mathbb{R}^{N \times n}$, where $A_{ij}^s = A_{is_j}$ for $1 \leq i \leq N, 1 \leq j \leq n$. The bi-adjacency matrix is applied to represent the connections related to the selected node set V_s . In the SBM framework, nodes within a community often have a similar connection intensity to the selected nodes, whereas nodes in different communities have a different connection intensity from the selected nodes. For instance, we display a graph with ten nodes and two communities as shown in the left panel of Figure 2, where the selected nodes are gray. The right panel shows the transpose of bi-adjacency matrix $(A^s)^\top$. There are clear block structures in the bi-adjacency matrix, and nodes within a community are gathered in the same block. Therefore, based on the proper selected node set, the bi-adjacency matrix can contain almost all network community structure information. Then, we apply spectral clustering to the normalized bi-adjacency matrix. Considering that, for adjacency matrix A , its normalized Laplacian matrix can be denoted by $L = D^{-1/2}AD^{-1/2} \in \mathbb{R}^{N \times N}$, where D is a diagonal matrix with the i -th diagonal element being $\sum_j A_{ij}$, ($1 \leq i \leq N$). Then, a sampled Laplacian (normalized bi-adjacency) matrix can be defined as

$$L^s = (D_{(r)}^s)^{-1/2}A^s(D_{(c)}^s)^{-1/2} \in \mathbb{R}^{N \times n}, \quad (2.1)$$

where $D_{(r)}^s = \{\sum_j A_{ij}^s\} \in \mathbb{R}^{N \times N}$ and $D_{(c)}^s = \{\sum_i A_{ij}^s\} \in \mathbb{R}^{n \times n}$ are defined as the out- and in-degree matrices of subsampled node set V_s , respectively.

We next discuss how to obtain embedding vectors for the entire network based on

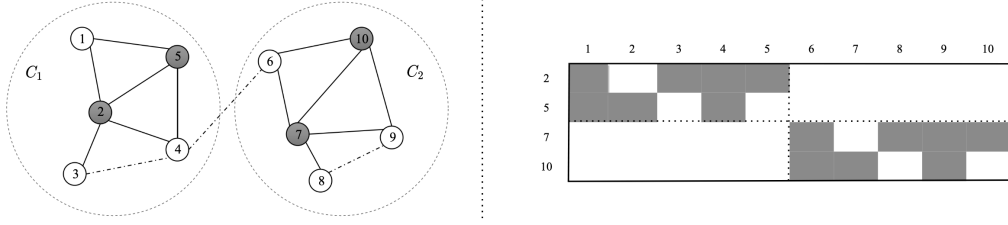


Figure 2: An illustration of a bi-adjacency matrix. The left panel displays a graph with ten nodes, two communities (C_1, C_2) and four selected nodes indicated by gray. The right panel represents the transpose of the bi-adjacency matrix, $\{A^s\}^\top$, where the gray scale indicates that there is an edge between the corresponding pair of nodes.

the subsampled Laplacian matrix. Assume that the SVD of L^s could be expressed as $L^s = U^s \widehat{\Sigma}^s V^\top \in \mathbb{R}^{N \times n}$, where $\widehat{\Sigma}^s \in \mathbb{R}^{n \times n}$ is a diagonal matrix with the eigenvalues of L^s sorted in decreasing order. Let $U^s \in \mathbb{R}^{N \times n}$ and $V \in \mathbb{R}^{n \times n}$ denote the corresponding left and right eigenvector matrices, respectively. As a result, the SVD decomposition of $(L^s)^\top L^s \in \mathbb{R}^{n \times n}$ can be denoted as follows: $(L^s)^\top L^s = V(\widehat{\Sigma}^s)^2 V^\top = V \widehat{\Lambda} V^\top$, where $\widehat{\Lambda} = (\widehat{\Sigma}^s)^2$. Then, we have $U^s = L^s V (\widehat{\Lambda}^{1/2})^\dagger$, where M^\dagger is defined as the pseudo-inverse matrix of an arbitrary matrix, M . Furthermore, let $\widehat{U}_K \in \mathbb{R}^{N \times K}$ be the matrix containing left K eigenvectors of L^s corresponding to its largest K eigenvalues. Then,

$$\widehat{U}_K = L^s V_K (\widehat{\Lambda}_K^{1/2})^\dagger, \quad (2.2)$$

where $\widehat{\Lambda}_K^{1/2} \in \mathbb{R}^{K \times K}$ is defined as a diagonal matrix with the K largest eigenvalues of $(L^s)^\top L^s$ and V_K is a matrix that contains the right K eigenvectors of $(L^s)^\top L^s$ corresponding to its largest K eigenvalues. We consider \widehat{U}_K as the approximated embedding vectors of all network nodes. Then, community membership can be obtained by applying the k-means algorithm to the rows of \widehat{U}_K . Additionally, the partition results are recorded by $\widehat{C}_k = \{i : \hat{z}_i = k, 1 \leq i \leq N\} (k = 1, \dots, K)$, where \hat{z}_i is the estimate label of node i . For simplicity, the extension of a spectral clustering algorithm by subsampling is referred to as the SSC method. The following proposition describes the

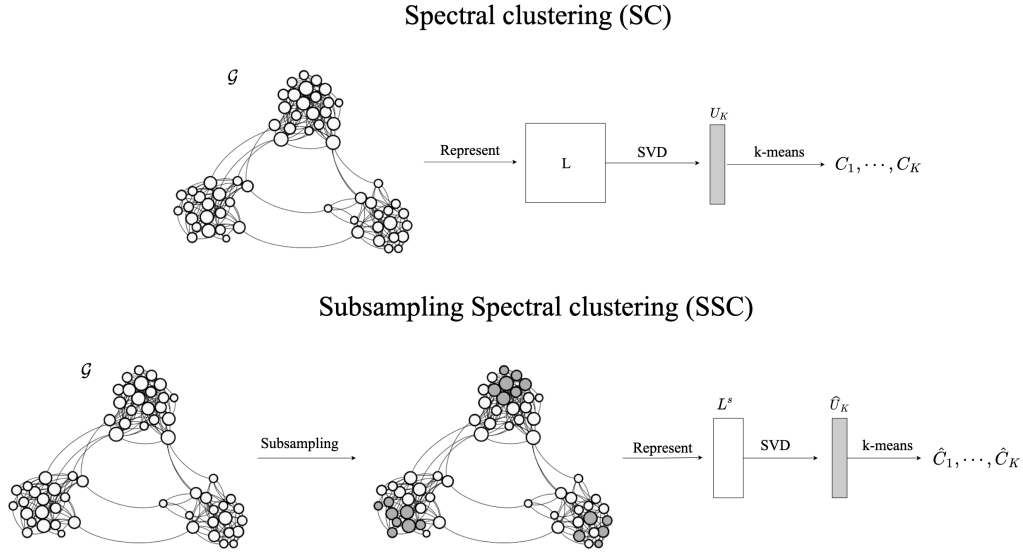


Figure 3: Comparison between spectral clustering and SSC. The upper panel represents the spectral clustering algorithm, which applies the k-means algorithm to the rows of the largest K eigenvectors of L (i.e., U_K) to obtain the clustering results. The lower panel shows the SSC algorithm, which applies subsampling to extract a subset of the entire node set where the gray nodes are the selected ones. Then, we form a subsampled Laplacian matrix L^s , and, through spectral analysis, we find its largest K left eigenvectors, \hat{U}_K . We also apply the k-means algorithm to the rows of \hat{U}_K to obtain the clustering results.

computational complexity of this method.

Proposition 1. (Computational Complexity) *For a graph \mathcal{G} with N nodes, assume that n nodes are subsampled from \mathcal{G} . Then, the computational complexity of community detection for the entire graph, \mathcal{G} , based on the SSC algorithm is $O(n^2N)$.*

The proof of Proposition 1 is provided in Appendix B.1 of the Supplementary Material. Compared with that of the traditional spectral clustering method based on the entire network, the computational complexity of the SSC is significantly lower. Proposition 1 shows that, for limited computing resources, the SSC algorithm could be applied to reduce the computational burden of community detection for large-scale networks.

To further illustrate the proposed method, we compare SSC with the traditional spectral clustering algorithm for the entire network in Figure 3. Evidently, unlike the

Algorithm 1 Subsampling Spectral Clustering

Input: graph \mathcal{G} , adjacency matrix $A \in \mathbb{R}^{N \times N}$, subsample node set $V_s = \{s_j : s_j \in [N], 1 \leq j \leq n\}$, number of communities K ;

1. Form bi-adjacency matrix $A^s \in \mathbb{R}^{N \times n}$ and compute its subsampled Laplacian matrix, $L^s \in \mathbb{R}^{N \times n}$, as defined in (2.1);
2. Conduct the SVD on $(L^s)^\top L^s$ and find its largest K eigenvalues and the corresponding eigenvectors;
3. Compute the approximation embedding vectors, \hat{U}_K , as defined in equation (2.2);
4. Conduct k-means to cluster the rows of \hat{U}_K into K clusters $\hat{C}_1, \dots, \hat{C}_K$.

Output: partition results $\hat{C}_1, \dots, \hat{C}_K$.

traditional spectral clustering method, SSC creates a subsampled Laplacian matrix with a much lower column dimension based on the small subsample. In other words, SSC is conducted on a small part of the connections in the entire network. Consequently, its clustering results may not be as accurate as those obtained by spectral clustering. However, it can obtain cluster labels for the entire network with limited computing resources. This could make network clustering feasible even using a personal computer.

The SSC procedure is described in Algorithm 1 and has several advantages. First, it overcomes the challenges of handling large-scale networks with limited computing resources. We only focus on selected nodes that are generated by subsampling and can identify the community structure using the connection information between the selected and entire node sets. Second, it is more flexible than classical spectral clustering because we can control subsample size n to balance accuracy and computational cost. Third, the SSC method is highly efficient. With a small subsample size, SSC can almost perfectly identify the community labels for all network nodes. This will be demonstrated in detail in the next few sections.

Remark 1 (Choosing the number of clusters). *Here, we discuss how to choose the number of clusters, K . Inspired by [Von Luxburg \(2007\)](#), the eigengap heuristic can be adopted in the SSC algorithm. Let $\hat{\lambda}_1 \geq \hat{\lambda}_2 \geq \dots \hat{\lambda}_n$ denote eigenvalues of the subsampled Laplacian matrix. The eigengap heuristic aims to identify the value of K satisfying that all $\hat{\lambda}_1, \dots, \hat{\lambda}_K$ are large enough, but $\hat{\lambda}_{K+1}$ is small. Specifically, an appropriate number of clusters can be obtained by the following three steps. First, we compute the eigenvalues of L^s and sort them in descending order. Second, we generate sequence $W = (w_1, \dots, w_{n-1})^\top \in \mathbb{R}^{n-1}$, where $w_k = \hat{\lambda}_k - \hat{\lambda}_{k+1}$ for $k = 1, 2, \dots, n-1$. Finally, we select K satisfying $K = \operatorname{argmax}_k w_k$ as the appropriate number of clusters.*

Intuitively, the subsampling method could affect the performance of the SSC. Next, we discuss two different subsampling methods and their corresponding theoretical properties.

2.2. Two Subsampling Methods

Here, we introduce two subsampling methods for spectral clustering under the SBM theoretical framework. In SBM, the link probabilities between node pairs depend only on their communities. Then, in terms of network structure information, the nodes in the same community have equal importance. Further, there are apparent differences in connection strength within and between communities. We first discuss SRS, and then, based on the stochastic block model, we design the DCS.

Simple random sampling is a uniform subsampling method, where the subsampling distribution is $p_i = n/N$ for $i = 1, 2, \dots, N$. We choose the nodes accordingly to obtain a subsampled node set V_s from \mathcal{G} in the first step. Then, using the SSC, the network clustering results can be obtained as desired. For simplicity, we refer to this procedure as the SRS-SC. According to [Vitter \(1985\)](#), the computational complexity

of subsampling by SRS is $O(N)$. Therefore, by Proposition 1, the computational complexity of SRS-SC is also $O(n^2N)$.

As previously discussed, our proposed method depends on selected node set V_s . Ideally, an informative subsample should have the following two properties. First, node set V_s contains nodes from K different blocks. Second, the nodes in V_s have dense connections with the unselected nodes to ensure that the set contains more network structure information. However, we cannot always generate a subsample like this by using SRS. This motivates us to design a degree-corrected subsampling spectral clustering algorithm.

Considering the properties of the SBM, all nodes within the same community have the same degree distribution. Therefore, the degrees of nodes provide important network structure information. For robustness, we regularize the node degree sequence. That is, we define a regularized degree sequence as $\hat{f}_i = \hat{d}_i/N$, where $\hat{d}_i = \sum_j A_{ij}$ is the observed degree of the i -th node, for $i = 1, 2, \dots, N$. Then, for an observed network, we have an initial node set partition using the k-means algorithm to the regularized degree sequence. We denote this initial partition as C_1^0, \dots, C_K^0 , where C_k^0 is the node set of the k -th cluster and $\bigcup_{k=1}^K C_k^0 = [N]$. Next, we sample the node set from C_1^0, \dots, C_K^0 . To collect more network connection information, for $k = 1, \dots, K$, we sort the nodes in the k -th cluster C_k^0 according to their regularized degrees in decreasing order. Then, we take the first $n|C_k^0|/N$ nodes from sorted node set C_k^0 , where $|C_k^0|$ is the size of C_k^0 . Therefore, these selected nodes have more connections with the unselected nodes than the randomly selected nodes from this set. We refer to it as DCS.

To illustrate the intuition of the DCS method, we generate a network from SBM with 6,000 nodes and three communities and set the subsample size to $n = 300$. Here, the community labels of the nodes are generated from an independent multinomial

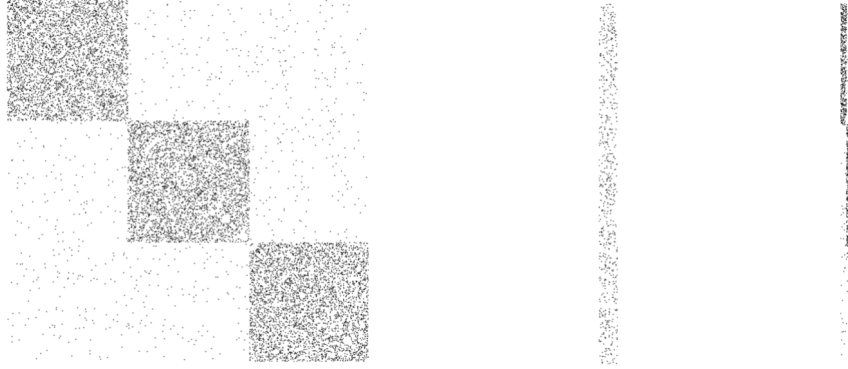


Figure 4: Plot of the adjacency matrix (left panel), bi-adjacency matrix formed by SRS (middle panel), and bi-adjacency matrix formed by DCS (right panel).

distribution with $\pi = (1/3, 1/3, 1/3)^\top$. For comparison, we plot the original adjacency and the bi-adjacency matrices formed by the SRS and DCS, respectively. The white color in these matrices indicates zero elements, and the black color non-zero elements. Furthermore, the rows and columns have been rearranged according to community structure. Evidently, according to the adjacency matrix (left panel), there are three blocks that represent three communities in this network. However, according to the middle panel of Figure 4, the community structure is not easy to identify based on the bi-adjacency matrix formed by SRS. Although the subsample node set covers three communities, the differences in the intensity connections within and between communities are unclear. In contrast with the SRS, there are clear boundaries for each block of the bi-adjacency matrix formed by the DCS. Since the connection intensity within blocks is significantly larger than that between blocks, the bi-adjacency matrix formed by DCS is more useful in identifying network communities. We theoretically prove this conclusion in the next section.

As previously discussed, the DCS method obtains the subsampled node set in two steps. The first step derives an initial partition using node degree information. It is

a tentative description of node heterogeneity. The second step is a refinement procedure, which helps extract relatively influential nodes in each cluster. In this way, the subsampled node set has clearer boundaries between community blocks. Furthermore, compared with SRS, DCS selects the subsampled nodes that have more connections with the unselected ones. The degree-corrected subsampling algorithm is presented in Algorithm 2.

Algorithm 2 Degree-Corrected Subsampling (DCS) Method.

Input: graph \mathcal{G} , adjacency matrix $A \in \mathbb{R}^{N \times N}$, sample size n , number of communities K ;

1. Compute regularized degree sequence $\hat{f}_i = 1/N \sum_j A_{ij}$, for $i = 1, \dots, N$;
2. Run k-means clustering to the regularized degree sequence to obtain the initial nodes partition, C_1^0, \dots, C_K^0 ;
3. Sort decreasingly each cluster's node according to node degree;
4. Form the subsampled node set V_s by choosing the first $n|C_k^0|/N$ nodes from node set C_k^0 for $k = 1, 2, \dots, K$.

Output: subsampled node set V_s .

In general, DCS outputs a subsampled node set, V_s . Then, the entire network partition results can be obtained by the SSC. For simplicity, this procedure is referred to as DCS-SC.

3. THEORETICAL PROPERTIES OF THE SSC ALGORITHMS

In this section, we first discuss the clustering accuracy of the the SRS-SC algorithm in three steps. First, we establish the theoretical properties of the SRS-SC algorithm based on population analysis. Second, we show the consistency of eigenvectors. Third, we provide the upper bound of the misclustered rate caused by the SRS-SC algorithm. Similarly, we could establish the theoretical properties of the DCS-SC.

3.1. Population Analysis of the SRS-SC Algorithm

For an observed network, we know that the SRS-SC algorithm is applied to the adjacency matrix. Population analysis implies that we discuss the theoretical properties of SRS-SC based on the SBM probability matrix defined as (3.1), rather than the adjacency matrix. Following the theoretical analysis techniques of Lei et al. (2015) and Joseph et al. (2016), we establish the properties of the SRS-SC algorithm based on population analysis. As a result, we establish that the embedding vectors obtained by the observed subsampled Laplacian matrix converges with those derived by the population subsampled Laplacian matrix. Then, the upper bound of the misclustered rate for the SRS-SC algorithm based on subsampled network data can be established as desired.

We introduce more network notations corresponding to the population subsampled Laplacian matrix as follows. We denote the SBM probability matrix (population adjacency matrix) as

$$\mathcal{A} = ZBZ^\top \in \mathbb{R}^{N \times N}, \quad (3.1)$$

where $Z \in \{0, 1\}^{N \times K}$ is a membership matrix, with each row having only one nonzero entry, $Z_{iz_i} = 1$. Then, the population Laplacian matrix is $\mathcal{L} = \mathcal{D}^{-1/2} \mathcal{A} \mathcal{D}^{-1/2}$, where \mathcal{D} is the degree matrix of \mathcal{A} . Similarly, under the SSC algorithm, the population biadjacency matrix is defined as $\mathcal{A}^s \in \mathbb{R}^{N \times n}$ and the corresponding subsampled Laplacian matrix as $\mathcal{L}^s = (\mathcal{D}_{(r)}^s)^{-1/2} \mathcal{A}^s (\mathcal{D}_{(c)}^s)^{-1/2} \in \mathbb{R}^{N \times n}$. Furthermore, the approximation embedding vectors are the largest K left eigenvectors of \mathcal{L}^s , denoted by $\hat{\mathcal{U}}_K$.

Then, we discuss the minimum sample size, n , required for subsampling. The estimation of the community labels relies on the connection information between the entire node set and the selected nodes. For accuracy, the selected node set should

contain nodes from all communities in the entire node set. Then, the desired situation is that the selected node set V_s has already contained nodes from K different blocks. Therefore, a desired event can be defined as $e = \{V_s : |V_s| = n; \forall k \in [K], \exists i \in V_s, z_i = k\}$.

Next, based on the population analysis, we provide the lower bound of the necessary sample size, n , to ensure that event e happens with high probability. Assume the block sizes of the entire network are N_1, \dots, N_K , respectively, satisfying $\sum_{k=1}^K N_k = N$. Define $N_{\min} = \min\{N_1, \dots, N_K\}$, and $\alpha = N_{\min}/N$. Under SBM with K blocks, assume the sample nodes are collected through simple random sampling with replacement. Then, we have the following proposition.

Proposition 2. (Required Subsample size) *For any $\epsilon > 0$, if subsample size is*

$$n \geq \frac{\log(K/\epsilon)}{\log\{1/(1-\alpha)\}},$$

event e happens with probability at least $1 - \epsilon$.

The proof of Proposition 2 is provided in Appendix B.2 of the Supplementary Material. Proposition 2 gives the lower bound of the subsampling size to ensure the subsampled node set V_s contains K blocks with high probability. It is noteworthy that the lower bound of subsample size n depends on two factors: (1) the number of blocks K and (2) the imbalance level of block size α . Specifically, if the network contains many blocks, subsample size n should be relatively large. Additionally, the imbalance level is negatively correlated with subsample size n . In this study, we consider imbalance level $\alpha = \Omega\{1/\log(N)\}$, where $\Omega\{g(N)\}$ means that, for the set of all $f(N)$, there exist positive constants a_0 and N_0 such that $f(N) \geq a_0 g(N)$ for all $N \geq N_0$ (Knuth, 1976). In this case, the required minimum sample size is $n = \Omega\{\log(1/\epsilon) \log(N)\}$. Ideally, if

the nodes are uniformly distributed among the different communities, the minimum required sample size is only $\Omega\{\log(1/\epsilon)\}$. This implies that, for a network with limited blocks and uniform block size, required sample size n can be quite small.

Next, we discuss the block structure of population approximation embedding vectors $\widehat{\mathcal{U}}_K$ obtained by using the SRS-SC method. The following proposition shows the connection between the membership matrix Z and population approximation embedding vectors $\widehat{\mathcal{U}}_K$.

Proposition 3. (Structure of Eigenvectors) *Assume that subsampled vertex set V_s is generated by simple random subsampling. If the sample size is $n \geq \frac{\log(K/\epsilon)}{\log\{1/(1-\alpha)\}}$, for any $\epsilon > 0$, there exists a matrix $\mu \in \mathbb{R}^{K \times K}$ such that $\widehat{\mathcal{U}}_K = Z\mu$. Furthermore,*

$$Z_i\mu = Z_j\mu \iff Z_i = Z_j,$$

with probability at least $1 - \epsilon$, where $Z \in \mathbb{R}^{N \times K}$ is a membership matrix and Z_i is the i the row of Z .

The proof of Proposition 3 is provided in Appendix B.3 of the Supplementary Material. From Proposition 3, the population approximation embedding vectors have exactly K distinct rows. More importantly, if the i -th and j -th rows of $\widehat{\mathcal{U}}_K$ are equal (i.e., $Z_i\mu = Z_j\mu$), nodes i and j belong to the same cluster. This is an important conclusion for the SSC algorithm. Recall that, in the SSC algorithm, k-means clustering is applied to the rows of observed embedding vectors $\widehat{\mathcal{U}}_K$. Then, under the mild conditions discussed in the next section, one can verify that $\widehat{\mathcal{U}}_K$ converges to $\widehat{\mathcal{U}}_K$. Therefore, $\widehat{\mathcal{U}}_K$ has roughly K distinct rows as well. Applying k-means clustering to $\widehat{\mathcal{U}}_K$, we can estimate the block membership matrix Z . Next, we establish the theoretical properties of SRS-SC empirically.

3.2. Upper Bound of the Mislustered Rate Based on the SRS-SC Algorithm

As previously discussed, we have shown that the population embedding vectors obtained by the SRS-SC algorithm have exactly K distinct rows. Next, we show the consistency of the largest K left eigenvectors of the empirical subsampled Laplacian matrix. Consequently, the upper bound of the misclustered rate caused by the SRS-SC algorithm can be established.

Before establishing the properties of SRS-SC in empirical level, we make the following assumptions.

(A1) (Imbalance Level) Assume the cluster size imbalance level $\alpha = \Omega\{1/\log(N)\}$;

(A2) (Required Subsample Size) Assume the subsampled size $n = \Omega(\{\log(N)\}^2)$;

(A3) (Network Sparsity) Assume that the minimum degree is $\delta_n = \min_i\{(\mathcal{D}_{(r)}^s)_{ii}\} \geq b_0n$, where $0 < b_0 < 1$ is a constant.

Assumption (A1) is introduced to specify the cluster size imbalance level, as also discussed by [Lei et al. \(2015\)](#). That is, we allow the sample sizes in different clusters to be of different orders to some extent. Assumption (A2) ensures that the requirement of [Proposition 2](#) is satisfied. For simplicity, we take $\epsilon = N^{-1/2}$. Typically, in a large-scale dataset, N is extremely large so that ϵ could be small enough. Assumption (A3) is a necessary condition to ensure the connection intensity between the entire node set and the subsampled node set. Let $b_0 = \min_{1 \leq k, k' \leq K} B_{kk'}$. One can verify that $\delta_n = \min_i\{(\mathcal{D}_{(r)}^s)_{ii}\} = \min_i\{\sum_{j=1}^n B_{z_i z_{s_j}}\} \geq nb_0$. Consequently, δ_n can grow almost linearly with n due to b_0 is a constant and $0 < b_0 < 1$. Based on these assumptions, we illustrate the convergence of eigenvectors in the next theorem.

Theorem 1. (Convergence of Eigenvectors) Assume $\lambda_1 \geq \dots \geq \lambda_K$ are the eigenvalues of subsampled Laplacian matrix \mathcal{L}^s . If Assumptions (A1)–(A3) are satisfied, there exists an orthogonal matrix $\mathcal{O} \in \mathbb{R}^{K \times K}$ such that

$$\|\widehat{U}_K - \widehat{U}_K \mathcal{O}\|_F \leq \frac{6\sqrt{6}}{\lambda_K} \sqrt{\frac{K \log\{4\sqrt{N}(N+n)\}}{\delta_n}} \quad (3.2)$$

with probability at least $(1 - N^{-1/2})^2$.

The proof of Theorem 1 can be found in Appendix B.5 of the Supplementary Material. To illustrate the estimation error bound given in (3.2), we provide the following explanations. First, the error bound is related to λ_K . According to Rohe et al. (2011), λ_K is the eigengap of \mathcal{L}^s . Moreover, they pointed out that the eigengap cannot be too small. An adequate eigengap ensures that the population embedding vectors can be estimated well. Second, the error bound is lower if minimum degree δ_n is higher. To reduce the upper bound of the distance between \widehat{U}_K and $\widehat{U}_K \mathcal{O}$, the subgraph generated by simple random subsampling cannot be too sparse. Thus, if λ_K can be lower bounded by a positive constant and $\delta_n \gg K \log(N)$, then we have $\|\widehat{U}_K - \widehat{U}_K \mathcal{O}\|_F = o_p(1)$. Third, the upper bound is also related to the number of clusters, K , and the subsample size, n . Recall that Proposition 2 implies that the subsample size n mainly depends on the imbalance level α . Therefore, if the number of clusters, K , and the imbalance level, α , are relatively large, it is difficult to identify the network communities. This conclusion is identical with the one of Lei et al. (2015).

Next, we focus on the clustering error of SRS-SC. First, we give a sufficient condition for a node to be clustered correctly. Subsequently, according to this condition, we define a misclustered set. Finally, we establish the upper bound of the size of the misclustered set in Theorem 2.

Let $c_i \in \mathbb{R}^K$ denote the centroid of the cluster, where the i -th row of \widehat{U}_K belongs to, for $i = 1, 2, \dots, N$. According to Proposition 3, $Z_i\mu$ is the centroid corresponding to the i -th row of \widehat{U}_K . Hence, if observed centroid c_i is closer to the population centroid $Z_i\mu$ than any other population centroid $Z_j\mu$ for all j with $j \neq i$, node i is considered correctly clustered. Specifically, we provide a sufficient condition for a node to be clustered correctly as follows.

Proposition 4. (Clustered Correctly) *Node i is clustered correctly, if*

$$\|c_i - Z_i\mu\mathcal{O}\| \leq \frac{1}{\sqrt{2N_{\max}}},$$

where $N_{\max} = \max\{N_1, \dots, N_K\}$ is the size of the largest block.

The proof of the Proposition 4 is provided in Appendix B.4 of the Supplementary Material. According to Proposition 4, we can define the misclustered node set as $\mathcal{R} = \{i : \|c_i - Z_i\mu\mathcal{O}\| > (2N_{\max})^{-1/2}\}$. Based on this definition, we then provide the upper bound of misclustered rate $|\mathcal{R}|/N$.

Theorem 2. (Upper Bound of the Misclustered Rate) *Assume that Assumptions (A1)-(A3) are satisfied. Then, there exists a constant c_0 such that*

$$\frac{|\mathcal{R}|}{N} \leq \frac{c_0 N_{\max} K \log \{4\sqrt{N}(N+n)\}}{Nn\lambda_K^2}, \quad (3.3)$$

with probability at least $(1 - N^{-1/2})^2$.

The proof is provided in Appendix B.6 of the Supplementary Material. According to Theorem 2, we can draw the following conclusions. First, by (3.3), the misclustered rate decreases as the subsample size n increases. Second, in the special case of balanced

community sizes (i.e., $KN_{max} = O(N)$) and positive constant K and λ_K , if $n \geq \{\log(N)\}^2$, then $|\mathcal{R}|/N = O\{\log(N)^{-1}\}$.

3.3. Theoretical Analysis of the DCS-SC Algorithm

For simplicity, we introduce some necessary notations as follows: recall that the observed regularized degree sequence is $\hat{f}_i = N^{-1} \sum_j A_{ij}$, $i = 1, 2, \dots, N$. Under the SBM, these are independent random variables with expectation $f_i = E(\hat{f}_i)$ for $i = 1, 2, \dots, N$. The matrix expression can be denoted by $\hat{F} = (\hat{f}_1, \dots, \hat{f}_N)^\top$, $F = (f_1, \dots, f_N)^\top \in \mathbb{R}^N$. Consider that the DCS algorithm applies k-means clustering to the regularized degree sequence, $\hat{f}_1, \dots, \hat{f}_N$, in the first step. Let \hat{F}_k denote the centroid of the k -th cluster for $k = 1, 2, \dots, K$. Further, define $\Delta_k = N_k^{-1/2} \|\hat{F}_k - F\| = \sqrt{\sum_i (\hat{f}_i - f_i)^2 / N_k}$. Then, the detailed assumptions are as follows:

- (A1) (Degree Blocks) Assume that the expectation of regularized degree sequence F contains exactly K distinct elements. Moreover, for $k = 1, 2, \dots, K$ and $i = 1, 2, \dots, N$, if $z_i = k$, let $F_k = f_i$;
- (A2) (Separation Condition) Assume that, for any $1 \leq k, k' \leq K$, $k \neq k'$, $|F_k - F_{k'}| \geq c(N_k^{-1/2} + N_{k'}^{-1/2}) \|\hat{F} - F\|$, where c is a large constant.

Assumption (A1) is introduced to ensure that the degree sequence can be partitioned into distinct K blocks. Further, assume the stochastic block model is defined as in (4.1). Then, the elements of F can be expressed as $f_i = (N - N_{z_i})\beta\zeta + (N_{z_i} - 1)\beta = \beta\{(N\zeta - 1) + N_{z_i}(1 - \zeta)\}$, for $i = 1, 2, \dots, N$. Therefore, under this condition, if the block sizes N_1, \dots, N_K are different, Assumption (A1) can be satisfied. Assumption (A2) is widely used to ensure the good performance of the k-means clustering algorithm

(Awasthi and Sheffet, 2012). Under the above assumptions, we posit the following proposition on the required subsample size of the DCS-SC.

Proposition 5. (Required Subsample Size) *Under an SBM with K blocks, assume the sample nodes are obtained by the DCS algorithm. For any $\epsilon > 0$, if Assumptions (A1)-(A2) are satisfied and the subsample size is $n \geq 64 \log(2N\epsilon^{-1})$, event e happens with probability at least $1 - \epsilon$.*

The proof of Proposition 5 can be found in Appendix C.1 of the Supplementary Material. Proposition 5 implies that, by the DCS algorithm, if the subsample size is $n = \Omega\{\log(N)\}$, the subsample node set can contain nodes from all network blocks with high probability. Intuitively, the DCS algorithm collects network structure information more effectively than that of SRS. Next, we establish the upper bound of the misclustered rate caused by the DCS-SC algorithm.

Theorem 3. (Misclustered Rate) *From Assumptions (A1)-(A2), if subsample size $n \geq 24 \log(2N)$ and the minimum expected average degree $\delta_n = \min_i\{(\mathcal{D}_{(r)}^s)_{ii}\}$ satisfy Assumption (A3), there exists a constant c_1 such that*

$$\frac{|\mathcal{R}|}{N} \leq \frac{c_1 N_{\max} K \log\{4\sqrt{N}(N+n)\}}{Nn\lambda_K^2},$$

with probability at least $(1 - N^{-1/2})^2$.

As the proof of Theorem 3 is similar to that of Theorem 2, we omit a detailed proof here. According to Theorem 3, the required subsample size for the DCS-SC is $n \geq 24 \log(2N)$, while the required subsampled size for the SRS-SC is $n = \Omega(\{\log(N)\}^2)$. More importantly, the misclustered rate of the DCS-SC has the same convergence rate as that of the SRS-SC. This demonstrates that the DCS-SC can be more effective than the SRS-SC.

4. NUMERICAL STUDIES

In this section, we present three simulation scenarios to examine the performances of both the DCS-SC and SRS-SC. Then, we demonstrate the performance of our proposed methods using a Sina Weibo dataset.

4.1. Simulation Models and Performance Measurements

In the simulation studies, we use the SBM model to generate networks with $K = 3$ communities. The block matrix B is controlled by two parameters β and ζ and is constructed as follows:

$$B = \beta\{(1 - \zeta) * I_K + \zeta \mathbf{1}_K \mathbf{1}_K^\top\}, \quad (4.1)$$

where $\beta \in [0, 1]$ is the connection intensity, $\zeta \in [0, 1]$ is the connection out-in-ratio, $I_K \in \mathbb{R}^{K \times K}$ is an identity matrix, and $\mathbf{1}_K \in \mathbb{R}^K$ is filled with elements 1. Additionally, the community labels of the nodes are generated from an independent multinomial distribution with $\pi \in \mathbb{R}^K$.

SCENARIO 1 (Consistency of the SSC) We set $\beta = 0.1$, $\zeta = 0.05$ and $\pi = (1/3, 1/3, 1/3)^\top$. Then, to demonstrate the consistency of the SSC algorithm, we let the size of network N grow from 5,000 to 30,000. Moreover, according to Theorems 2 and 3, for each setting of N , we set n to be $\lceil 2\{\log(N)\}^2 \rceil$, where $\lceil x \rceil$ is the smallest integer greater than or equal to a real number x .

SCENARIO 2 (Effect of Subsample Size on the SSC) We set $N = 12,000$, $\beta = 0.03$, $\zeta = 0.05$ and $\pi = (1/3, 1/3, 1/3)^\top$. To reflect the impact of subsample size, n is set to vary from 100 to 1,100.

SCENARIO 3 (Effect of Signal Strength on the SSC) According to the SBM block matrix defined in (4.1), the signal strength of community membership depends

on β and ζ . Here, we fix $N = 12,000$ and $n = 100$ and set the multinomial distribution as $\pi = (1/3, 1/3, 1/3)^\top$. Then, to examine the impact of β and ζ , we set β to increase from 0 to 0.95. Correspondingly, ζ increases from 0 to 0.95.

SCENARIO 4 (Effect of Imbalance on the SSC) Under this scenario, we fix the network size $N = 12,000$, $n = 100$, $\beta = 0.1$ and $\zeta = 0.05$. To reflect the imbalance of the network cluster, we set $\pi = (1/3 - \Delta, 1/3, 1/3 + \Delta)^\top$ with Δ varying from 0 to 0.3, where a larger Δ implies greater imbalance in the cluster size.

To evaluate clustering performance, we consider the misclustered rate, which has been widely used in the investigation of community detection under SBM (Gao et al., 2018). Let $\hat{Z} \in \mathbb{R}^{N \times K}$ be the estimated membership matrix. Then, the misclustered rate is calculated as

$$\mathcal{R}(\hat{Z}, Z) = \frac{1}{N} \min_{\mathcal{O} \in \mathbb{E}_K} d(\hat{Z}\mathcal{O}, Z) \quad (4.2)$$

where \mathbb{E}_K is the set of all $K \times K$ permutation matrices and $d(\cdot, \cdot)$ is the distance function of two matrices with the same dimension. It counts the number of different rows between these two matrices, that is, $d(\hat{Z}, Z) = \sum_{i=1}^N \mathbb{I}(\hat{Z}_i \neq Z_i)$, where $\mathbb{I}(\cdot)$ is an indicator function. For a reliable evaluation, the random experiments are repeated for $T = 100$ times. All simulations are conducted in Python using a Dell computer with a 3.70 GHz Intel Core i9 processor.

4.2. Simulation Results

The detailed results are represented in Figures 5–8. We can draw the following conclusions based on the simulation results.

SCENARIO 1. The result of Scenario 1 is shown in Figure 5. We could draw the following conclusions. First, as N increases, the misclustered rates of both the SRS-SC

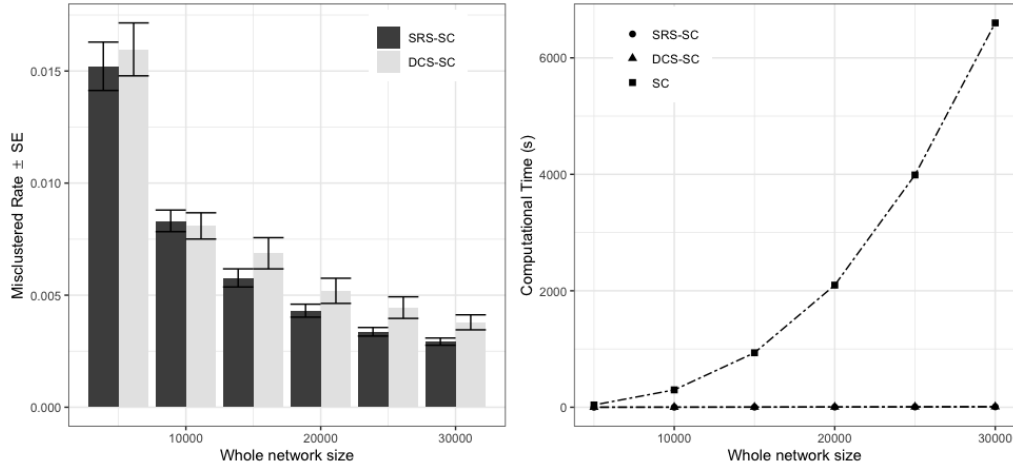


Figure 5: The misclustered rate (left panel) N grows from 5,000 to 30,000. Here, the subsample size is $n = \lceil 2\{\log(N)\}^2 \rceil$. Further, the standard error (SE) is reported by the error bar in the left panel. The average computational time (right panel) of the SRS-SC, DCS-SC, and SC are further compared as N increases.

and DCS-SC decrease, becoming close to 0. Moreover, Figure 5 shows that the standard errors of these two algorithms also decrease as N grows. Second, as we can observe from the right panel of Figure 5 that, as network size increases, the computational time of SC increases drastically compared with the SRS-SC and DCS-SC. These results not only support the theoretical conclusions of Theorems 2 and 3 but also justify our motivation and intuition to conduct the SSC.

SCENARIO 2. Figure 6 indicates the impact of n on the performance of the SRS-SC and DCS-SC. First, as the subsample size n grows, misclustered rates of these two algorithms decrease. Second, as shown in Figure 6, when $n = 300$, the misclustered rates of the SRS-SC and DCS-SC are both below 0.100, but the average computational time of these two algorithms is no greater than 2.000s. As a result, both the SRS-SC and DCS-SC could be applied in large-scale networks for community detection. This corroborates the theoretical findings in Theorems 2 and 3.

SCENARIO 3. Figure 7 and Table 1 show the performance of the methods when the signal strength varies. First, as presented in Table 1, the performances of these

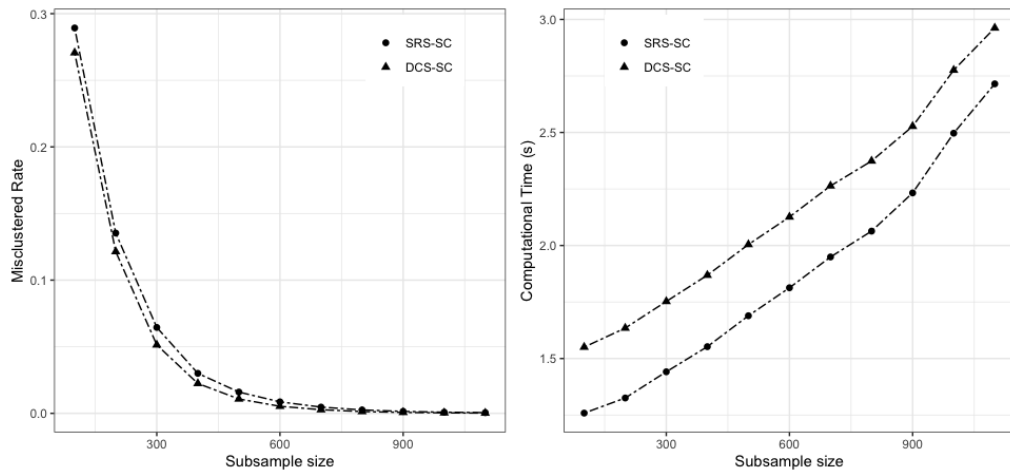


Figure 6: Impact of subsample size n on the performance of the SRS-SC and DCS-SC. The subsample size n varies from 100 to 1,100. Left panel: relationship between the misclustered rate and the subsample size n . Right panel: computational time versus the subsample size n .

Table 1: Simulation results of the SRS-SC and DCS-SC with β and ζ varying from 0.05 to 0.95. The misclustered rate of the SRS-SC and DCS-SC is reported accordingly. In addition, the standard error (SE) of misclustered rate is reported between parentheses.

| $\beta \setminus \zeta$ | | 0.05 | 0.35 | 0.65 | 0.95 |
|-------------------------|--------|------------|------------|------------|------------|
| 0.05 | SRS-SC | .173(.005) | .421(.042) | .620(.008) | .661(.001) |
| | DCS-SC | .169(.004) | .347(.002) | .610(.007) | .661(.001) |
| 0.35 | SRS-SC | .000(.000) | .024(.001) | .286(.038) | .656(.002) |
| | DCS-SC | .000(.000) | .025(.001) | .220(.002) | .657(.001) |
| 0.65 | SRS-SC | .000(.000) | .000(.000) | .060(.003) | .647(.003) |
| | DCS-SC | .000(.000) | .001(.000) | .057(.001) | .646(.002) |
| 0.95 | SRS-SC | .000(.000) | .000(.000) | .000(.000) | .541(.011) |
| | DCS-SC | .000(.000) | .000(.000) | .001(.000) | .546(.003) |

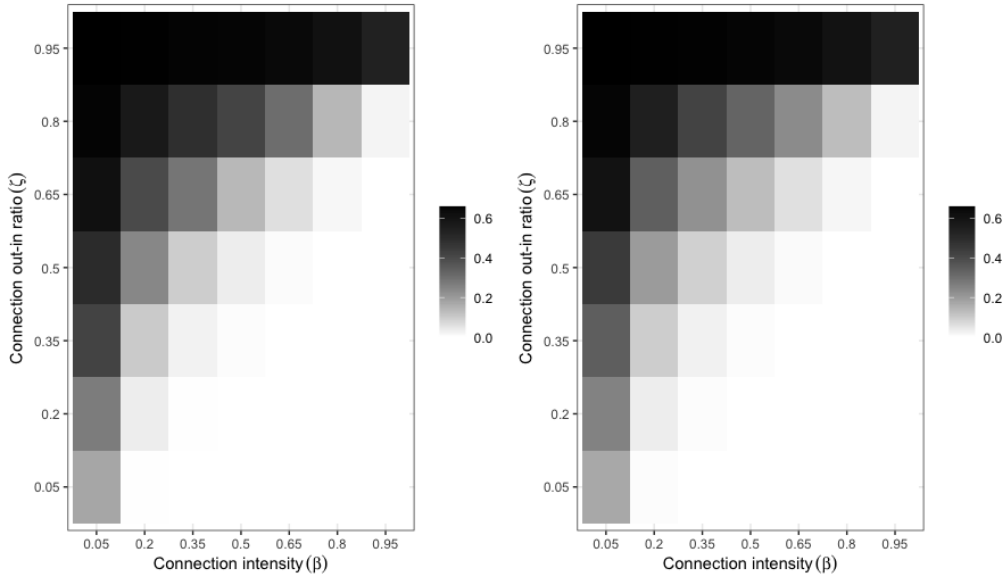


Figure 7: The effect of β and ζ under SRS-SC (left panel) and DCS-SC (right panel). The average misclustered rate is represented by the gray scale. Evidently, a stronger connection intensity and smaller connection out-in-ratio yield more accurate clustering results for these two methods.

two methods are satisfactory, except that the connection strength β is extremely small or the connection out-in-ratio ζ is very large. This means that, faced with fuzzy community structures and sparse scenarios, the subsample size needs to be increased appropriately for more accurate community detection. Second, for $\beta = 0.95$, as ζ decreases from 0.95 to 0.05, the misclustered rates of the SRS-SC and DCS-SC both drop to 0.000. Moreover, for $\zeta = 0.05$, as β varies from 0.05 to 0.95, the misclustered rates of these two methods decrease to 0.000. The results verify the theoretical conclusions of Theorems 2 and 3. Namely, the misclustered rate decreases as the signal strength increases. This phenomenon is also confirmed by Figure 7.

SCENARIO 4. Figure 8 shows that different imbalance levels have different effects on the performance of the SRS-SC and DCS-SC. First, as Δ increases from 0 to 0.1, the misclustered rates of these two methods increase. As Δ increases slightly, it is difficult to cover all communities with a small subsample size. Second, as Δ increases from

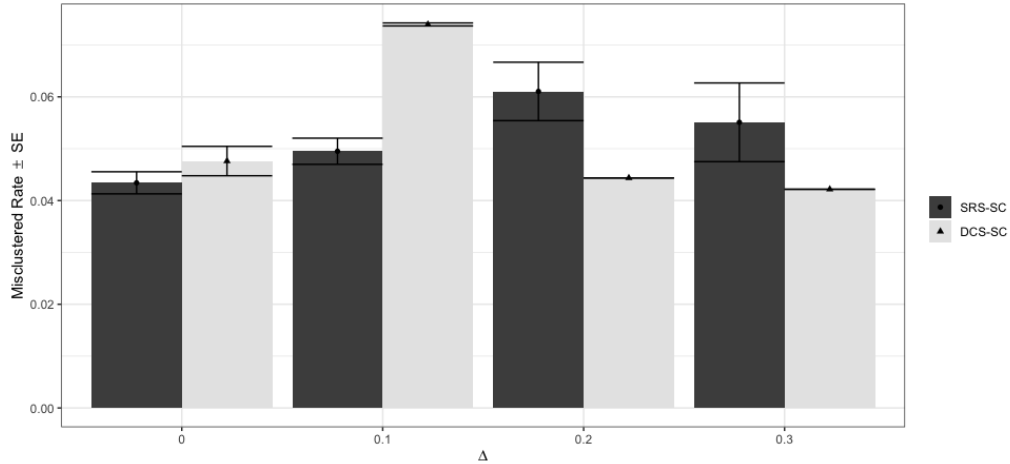


Figure 8: Simulation results of the SRS-SC and DCS-SC for the subsample size of Δ varying from 0 to 0.3. The misclustered rates of the SRS-SC and DCS-SC are reported accordingly. In addition, the standard error (SE) is reported by the error bar.

0.1 to 0.3, the misclustered rate of the DCS-SC declines. However, that of the SRS-SC increases initially and then decreases. Since the difference in the degree of nodes between communities becomes larger, DCS can collect more informative subsamples. Moreover, community structure is more clearly represented by the bi-adjacency matrix. Finally, the standard error of the DCS-SC drops to 0.000 as Δ increases. Therefore, for high imbalance cases, the DCS-SC obtains more stable and accurate clustering results.

Based on the empirical performance of SSC on these simulation studies, our proposed method is efficient and robust for analyzing large-scale networks. Additionally, the DCS method is more recommended for selecting a small node set from the entire network.

4.3. A Sina Weibo Dataset

We evaluate the SSC using a dataset collected from Sina Weibo (*www.weibo.com*), one of the largest Twitter-type social networks in China. Each node is a user, and an edge exists if there is a follower–followee relationship between two users. An undirected network is constructed based on this dataset. Given any two users, i and j , the

corresponding element of adjacency matrix A_{ij} is set to 1 if there is at least one edge between two users. This network has $N = 9,980$ nodes and $1,325,604$ undirected edges. The density of the network is $|E|/\binom{N}{2} = 0.027$, where $|E|$ denotes the number of edges.

It is noteworthy that, since the true community labels are unknown in the real data analysis, the misclustered rate is defined to measure the dissimilarity of community assignments between the entire network spectral clustering results and the SSC algorithms. According to the eigengap method discussed in Remark 1, the number of communities is selected as $K = 3$. Here, we set the subsample size $n = 200$ for both the SRS-SC and DCS-SC. Let $\tilde{Z} \in \mathbb{R}^{N \times K}$ denote the community membership matrix obtained by spectral clustering. Accordingly, let $\hat{Z} \in \mathbb{R}^{N \times K}$ denote the estimated membership matrix obtained by the SSC. Then, the misclustered rate is calculated by $\mathcal{R}(\hat{Z}, \tilde{Z}) = N^{-1} \min_{\mathcal{O} \in \mathbb{E}_K} d(\hat{Z}\mathcal{O}, \tilde{Z})$ defined as in (4.2).

We demonstrate the clustering results of both the spectral clustering and SSC methods. First, Figure 9 shows that the embedding vectors of network nodes have a clear community structure. This indicates that spectral clustering is feasible for identifying the community membership of this network. Second, the misclustered rate of the SRS-SC is 0.179, and the computational time is 0.404s, while the computational time of spectral clustering based on the entire network is 298.827s. For even larger networks, the SSC method is feasible even using a personal computer to obtain the cluster labels for the entire network. Finally, the average computational time of the DCS-SC is 0.674s and the misclustered rate of the DCS-SC is only 0.118. Namely, compared with the SRS-SC, the DCS-SC has higher clustering accuracy.

Furthermore, to determine more interesting information about the community structure obtained by the DCS-SC, we analyze the text information posted by the users of

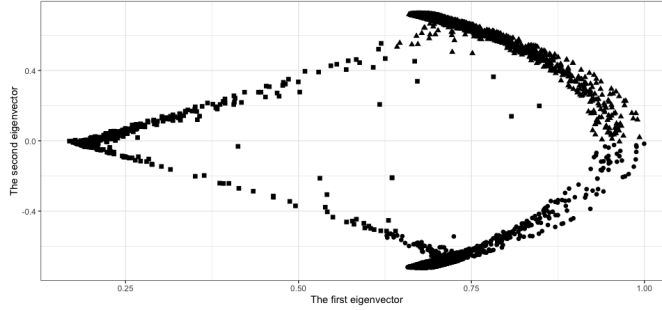


Figure 9: Largest two eigenvectors corresponding to the network Laplacian matrix. The x-axis provides the first largest eigenvector and the y-axis the second largest eigenvector values. The type of scattered points represents community label.

this social network. As shown in Figure 10, we plot three *word clouds* to depict the representative keywords of each community. The keywords of each community are generated by gathering the Sina Weibo content posted by users. The sizes of the keywords reflect word frequency, and the shapes of word clouds are related to high-frequency words. There are clear differences between the word clouds. Based on these word clouds, the members in different communities have distinct interests and play different roles in the network. The users assigned to the first cluster are highly concerned about the news, the high-frequency keywords of their blogs being “TV station” and “news.” The second cluster includes users who are interested in fashion and art, their high frequency keywords being “design,” “Brand,” and “works.” The third cluster is a group with a wide range of hobbies, and it has high-frequency keywords such as “League,” “film,” and “coffee.”

5. CONCLUDING REMARKS

In this study, we present an SSC algorithm to identify the community structure of large networks. Particularly, we discuss two subsampling methods (i.e., SRS and DCS). Theoretically, we investigate the subsample sizes for these two methods and establish the statistical properties of the clustering results. The computational complexity of the



Figure 10: Word clouds of the social network communities discovered by the DCS-SC. The shapes of word clouds represent the community label and the sizes of the words their frequencies. The left panel includes representative words related to news. The middle panel implies that the users are engaged in work about fashion and art. The right panel shows that the users in this community are used to sharing their leisure habits.

SSC algorithm can be reduced to $O(Nn^2)$, where n is the subsample size, which can be as low as $\Omega\{\log(N)^2\}$. Furthermore, the empirical results illustrate that we could identify 88.2% of the user community tags with only 0.2% of the time of the spectral clustering result based on the whole network.

The idea of the paper can be extended to research on other network data with more complex relationships, such as bipartite and multiple networks, which we are currently investigating. Additionally, here we study the subsampling method, which only needs to select the node set once. Another interesting issue in future research is to develop a multi-step subsampling method which can extract richer network structure information.

References

- Agarwal, S., Lim, J., Zelnik-Manor, L., Perona, P., Kriegman, D., and Belongie, S. (2005), “Beyond pairwise clustering,” in *2005 IEEE Computer Society Conference on Computer Vision and Pattern Recognition (CVPR’05)*, IEEE, vol. 2, pp. 838–845.
- Awasthi, P. and Sheffet, O. (2012), “Improved spectral-norm bounds for clustering,” in *Approximation, Randomization, and Combinatorial Optimization. Algorithms and Techniques*, Springer, pp. 37–49.
- Binkiewicz, N., Vogelstein, J. T., and Rohe, K. (2017), “Covariate-assisted spectral clustering,” *Biometrika*, 104, 361–377.
- Chen, J. and Yuan, B. (2006), “Detecting functional modules in the yeast protein–protein interaction network,” *Bioinformatics*, 22, 2283–2290.
- Chen, W.-Y., Song, Y., Bai, H., Lin, C.-J., and Chang, E. Y. (2010), “Parallel spectral clustering in distributed systems,” *IEEE Transactions on Pattern Analysis and Machine Intelligence*, 33, 568–586.
- Chen, X. and Cai, D. (2011), “Large scale spectral clustering with landmark-based representation,” in *Proceedings of the AAAI Conference on Artificial Intelligence*, vol. 25.
- Drineas, P. and Mahoney, M. W. (2005), “On the Nyström method for approximating a Gram matrix for improved kernel-based learning,” *The Journal of Machine Learning Research*, 6, 2153–2175.
- Feng, X., Yu, W., and Li, Y. (2018), “Faster matrix completion using randomized SVD,” in *2018 IEEE 30th International Conference on Tools with Artificial Intelligence (ICTAI)*, IEEE, pp. 608–615.

- Fortunato, S. (2010), “Community detection in graphs,” *Physics Reports*, 486, 75–174.
- Fowlkes, C., Belongie, S., Chung, F., and Malik, J. (2004), “Spectral grouping using the Nyström method,” *IEEE Transactions on Pattern Analysis and Machine Intelligence*, 26, 214–225.
- Gao, C., Ma, Z., Zhang, A. Y., Zhou, H. H., et al. (2018), “Community detection in degree-corrected block models,” *The Annals of Statistics*, 46, 2153–2185.
- Girvan, M. and Newman, M. E. (2002), “Community structure in social and biological networks,” *Proceedings of the National Academy of Sciences*, 99, 7821–7826.
- Halko, N., Martinsson, P.-G., and Tropp, J. A. (2011), “Finding structure with randomness: Probabilistic algorithms for constructing approximate matrix decompositions,” *SIAM Review*, 53, 217–288.
- Harenberg, S., Bello, G., Gjeltema, L., Ranshous, S., Harlalka, J., Seay, R., Padmanabhan, K., and Samatova, N. (2014), “Community detection in large-scale networks: a survey and empirical evaluation,” *Wiley Interdisciplinary Reviews: Computational Statistics*, 6, 426–439.
- Holland, P. W., Laskey, K. B., and Leinhardt, S. (1983), “Stochastic blockmodels: First steps,” *Social Networks*, 5, 109–137.
- Joseph, A., Yu, B., et al. (2016), “Impact of regularization on spectral clustering,” *The Annals of Statistics*, 44, 1765–1791.
- Knuth, D. E. (1976), “Big omicron and big omega and big theta,” *ACM Sigact News*, 8, 18–24.
- Krzakala, F., Moore, C., Mossel, E., Neeman, J., Sly, A., Zdeborová, L., and Zhang,

- P. (2013), “Spectral redemption in clustering sparse networks,” *Proceedings of the National Academy of Sciences*, 110, 20935–20940.
- Lancichinetti, A. and Fortunato, S. (2009), “Community detection algorithms: a comparative analysis,” *Physical Review E*, 80, 056117.
- Lee, S. H., Magallanes, J. M., and Porter, M. A. (2017), “Time-dependent community structure in legislation cosponsorship networks in the Congress of the Republic of Peru,” *Journal of Complex Networks*, 5, 127–144.
- Lei, J., Rinaldo, A., et al. (2015), “Consistency of spectral clustering in stochastic block models,” *The Annals of Statistics*, 43, 215–237.
- Li, M., Lian, X.-C., Kwok, J. T., and Lu, B.-L. (2011), “Time and space efficient spectral clustering via column sampling,” in *CVPR 2011*, IEEE, pp. 2297–2304.
- Martin, L., Loukas, A., and Vandergheynst, P. (2018), “Fast approximate spectral clustering for dynamic networks,” in *International Conference on Machine Learning*, PMLR, pp. 3423–3432.
- Nepusz, T., Yu, H., and Paccanaro, A. (2012), “Detecting overlapping protein complexes in protein-protein interaction networks,” *Nature Methods*, 9, 471–472.
- Newman, M. E. and Girvan, M. (2004), “Finding and evaluating community structure in networks,” *Physical Review E*, 69, 026113.
- Ng, A. Y., Jordan, M. I., and Weiss, Y. (2002), “On spectral clustering: Analysis and an algorithm,” in *Advances in Neural Information Processing Systems*, pp. 849–856.
- Rives, A. W. and Galitski, T. (2003), “Modular organization of cellular networks,” *Proceedings of the National Academy of Sciences*, 100, 1128–1133.

- Rohe, K., Chatterjee, S., Yu, B., et al. (2011), “Spectral clustering and the high-dimensional stochastic blockmodel,” *The Annals of Statistics*, 39, 1878–1915.
- Tron, R. and Vidal, R. (2007), “A benchmark for the comparison of 3-d motion segmentation algorithms,” in *2007 IEEE Conference on Computer Vision and Pattern Recognition*, IEEE, pp. 1–8.
- Vitter, J. S. (1985), “Random sampling with a reservoir,” *ACM Transactions on Mathematical Software (TOMS)*, 11, 37–57.
- Von Luxburg, U. (2007), “A tutorial on spectral clustering,” *Statistics and Computing*, 17, 395–416.
- Wang, H., Yang, M., and Stufken, J. (2019), “Information-based optimal subdata selection for big data linear regression,” *Journal of the American Statistical Association*, 114, 393–405.
- Wang, H., Zhu, R., and Ma, P. (2018), “Optimal subsampling for large sample logistic regression,” *Journal of the American Statistical Association*, 113, 829–844.
- Yan, D., Huang, L., and Jordan, M. I. (2009), “Fast approximate spectral clustering,” in *Proceedings of the 15th ACM SIGKDD International Conference on Knowledge Discovery and Data Mining*, pp. 907–916.
- Zhang, H., Guo, X., and Chang, X. (2022), “Randomized spectral clustering in large-scale stochastic block models,” *Journal of Computational and Graphical Statistics*, 0, 1–52.
- Zhao, Y., Levina, E., and Zhu, J. (2011), “Community extraction for social networks,” *Proceedings of the National Academy of Sciences*, 108, 7321–7326.